

# Mechanism of catalysis of the hydrolysis of a formamidine compound

2 PERKIN

Kevin N. Dalby

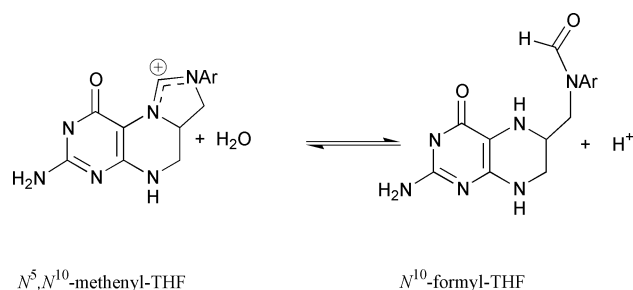
Division of Medicinal Chemistry, College of Pharmacy, University of Texas at Austin, TX 78712, USA and Graduate Programs in Biochemistry and Molecular Biology and the Center for Molecular and Cellular Toxicology. E-mail: Dalby@mail.utexas.edu; Fax: 512-232 2606; Tel: 512-471 9267

Received (in Cambridge, UK) 25th April 2001, Accepted 13th July 2001  
First published as an Advance Article on the web 29th August 2001

The hydrolysis of a fluoroformamidine ion to give a urea is subject to general base catalysis, where the addition of water is catalyzed by carboxylate monoanions ( $pK_a$  2.22–5.52) with a Brønsted coefficient of  $\beta = 0.80$  through a class n mechanism. The Brønsted coefficient and small solvent isotope effect of  $k_H/k_D = 1.2 \pm 0.2$  for catalysis by acetate anion are consistent with significant movement of a hydron towards the catalyst in a late asymmetric transition state. A concerted mechanism is proposed that is enforced by proton transfer within a hydrogen-bonded intermediate species, in which the difference in  $pK_a$  between the catalyst and the intermediate is  $\sim 16$  units. Hydroxide and carbonate deviate below an extrapolation through a series of carboxylate anions, suggesting that over a wider range of  $pK_a$  the Brønsted plot displays downward curvature, possibly due to a ‘Hammond effect’ on the proton transfer component of the reaction, that results in a change in transition-state structure with increasing  $pK_a$  of the base catalyst. A 30-fold positive deviation of the uncatalyzed reaction from the limiting Brønsted line through the carboxylates suggests that the uncatalyzed reaction occurs *via* a different mechanism. The solvent isotope effect of  $k_H/k_D = 1.7 \pm 0.1$  and Brønsted type coefficients (for donating nitrogen substituents) of  $\beta_{dg}^{ArN} = -0.3$  and  $\beta_{dg}^{RN} = -0.4$  for the uncatalyzed reaction are consistent with either a stepwise mechanism of addition and proton transfer, or a cyclic transition state containing two hydrogen bonded water molecules.

## Introduction

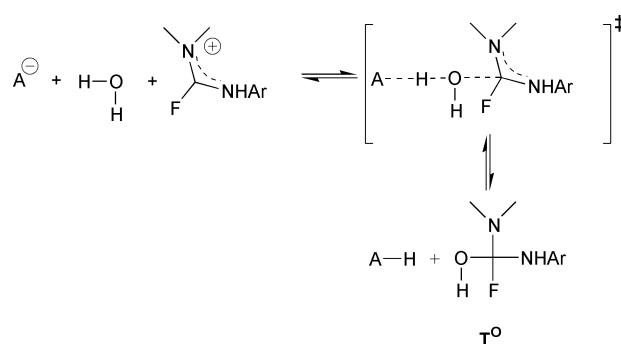
Tetrahydrofolate (THF) derivatives function as multioxidation state sources of monocarbon units in cells. They participate in a range of processes including the degradation and production of several amino acids, the biosynthesis of purine bases, and the biosynthesis of thymidylate.<sup>1</sup> The enzymes that control the metabolism of these derivatives are important for cell growth and are potentially attractive pharmaceutical targets. One transformation central to this process is the formation of  $N^{10}$ -formyl-THF by the hydrolysis of the amidinium moiety of  $N^5, N^{10}$ -methenyl-THF, which is catalyzed by the enzyme  $N^5, N^{10}$ -methenyl-THF cyclohydrolase (Scheme 1).



Scheme 1

While hydrolysis of the amidine group has been fairly extensively studied in acid and base solutions<sup>2,3</sup> and models of THF have been examined in considerable detail,<sup>4–10</sup> factors contributing to the *formation* of reaction intermediates, especially those pertaining to the enzyme-catalyzed reaction, have not been illuminated in such studies. Here a mechanistic study is described where general base catalysis through a class n mechanism<sup>11</sup> for the addition of water to a fluoroformamidine ion

is observed with extensive transfer of a hydron to the base at the transition state (Scheme 2). This study provides insight into one



Scheme 2

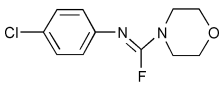
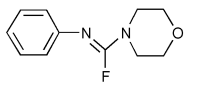
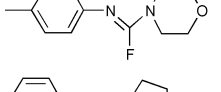
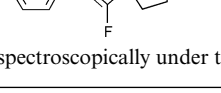
catalytic role of Lys-56 of cyclohydrolase, which is proposed to be the sole general acid–base residue in the active site of the enzyme.

## Results

### Spontaneous solvolysis

To investigate the pathways of fluoroformamide hydrolysis the pH dependence for the solvolysis of **1a** (See Table 1) was investigated. Rate constants for hydrolysis,  $k_{hyd}$ , were obtained from buffer-independent rate constants or where appropriate in dilute solutions of HCl or DCl. The pH–rate profile for the hydrolysis of **1a** in  $H_2O$  displays two distinct regions (Fig. 1). These are represented by the two terms in the rate law of eqn. (1), where S and  $SH^+$  represent fluoroformamide and a fluoroformamidine ion, respectively and which may be inter-

**Table 1** Equilibrium and rate constants for the hydrolysis of fluoroformamidines at 25 °C and ionic strength 1.0 M (KCl)

Compound	$K_a$	$k_1$	$k_0$
<b>1a</b> 	$2.6 \pm 0.2 \times 10^{-3}$	0.019	$1.8 \pm 0.3 \times 10^{-3}$
<b>1a</b> 	$(5.2 \pm 0.8 \times 10^{-4})^a$	$(0.011)^a$	$(1.8 \pm 0.3) \times 10^{-3a}$
<b>1b</b> 	$0.001^b$	0.01	0.00343
<b>1c</b> 	0.00016	0.0078 <sup>c</sup>	Not determined
<b>1d</b> 	Not determined	0.00064	0.00445

<sup>a</sup> Performed in D<sub>2</sub>O. <sup>b</sup> Measured spectroscopically under the standard kinetic conditions at 260 nm. <sup>c</sup> Obtained in 0.1 M HCl.

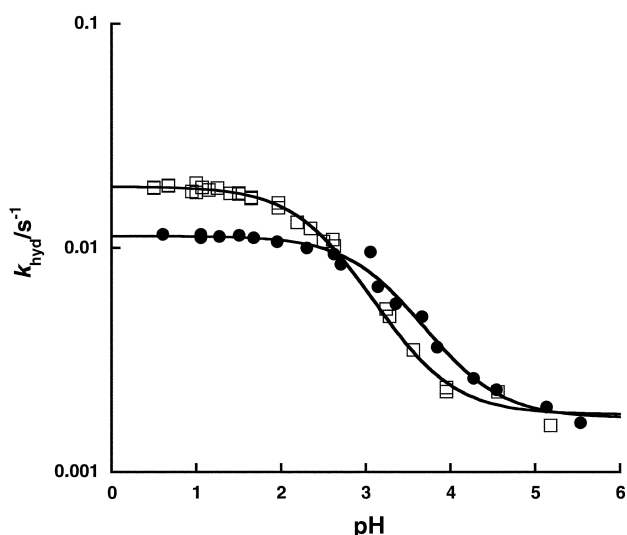
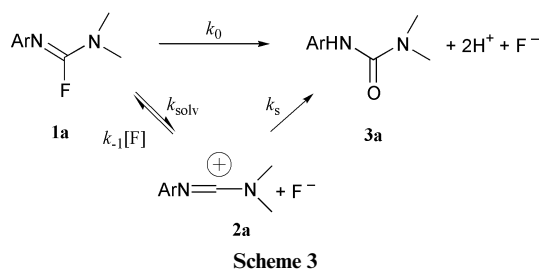


**Fig. 1** Dependence on pH of the first order rate constant,  $k_{\text{hyd}}$ , for the hydrolysis of **1** at 25 °C and ionic strength 1.0 M (KCl) in H<sub>2</sub>O (□) and D<sub>2</sub>O (●). The solid lines represent the best non-linear least squares fits through the data according to eqn (2);  $k_{\text{hyd}} = (k_1[\text{H}] + k_0K_a)/([\text{H}] + K_a)$  where  $k_1 = 0.0188 \text{ s}^{-1}$ ,  $k_0 = 0.0018 \pm 0.0002 \text{ s}^{-1}$  and  $K_a = 0.0026 \pm 0.0001$  in H<sub>2</sub>O (□) and  $k_1 = 0.0113 \text{ s}^{-1}$ ,  $k_0 = 0.0018 \text{ s}^{-1}$  and  $K_a = 0.00052$  in D<sub>2</sub>O (●). The data were obtained from extrapolation to zero buffer concentration of plots of  $k_{\text{obs}}$  against buffer concentrations for solutions where the pH or pD is above 2. Below pH 2 measurements were made in dilute solutions of HCl or DCl.

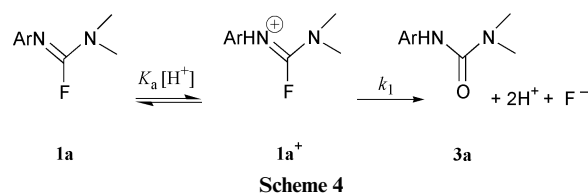
preted as described below. The pH-independent region above pH 5 corresponds to the term,  $k_0$ , in eqn. (1), and represents

$$k_{\text{hyd}} [\text{S}] = k_1[\text{SH}^+] + k_0[\text{S}] \quad (1)$$

unimolecular solvolysis of **1a** ( $k_{\text{solv}} = 0.0018 \text{ s}^{-1}$ ) through the iminium ion **2a** which is hydrolyzed in a fast step ( $k_s = 5.8 \times 10^5 \text{ s}^{-1}$ ) to give the urea **3a** (Scheme 3).<sup>12</sup>



Protonation of the amidine functional group (N=C-N) occurs on the imino nitrogen, to give the resonance stabilized



cation **1a<sup>+</sup>** (Scheme 4).<sup>13</sup> Below pH 5 the increase and subsequent plateau of  $k_{\text{hyd}}$  corresponds to the term  $k_1$  and represents hydrolysis of **1a<sup>+</sup>**. The kinetic parameters in eqn. (2) were

$$k_{\text{hyd}} = (k_1[\text{H}] + k_0K_a)/([\text{H}] + K_a) \quad (2)$$

obtained from non-linear least squares analysis of the pH–rate profiles for the solvolysis of **1a** in H<sub>2</sub>O and D<sub>2</sub>O shown in Fig. 1 and are presented in Table 1. A moderate solvent deuterium isotope effect of  $k_{\text{H}}/k_{\text{D}} = 1.7$  for the hydrolysis of **1a<sup>+</sup>** and an equilibrium solvent deuterium isotope effect of  $K_{\text{H}}/K_{\text{D}} = 5 \pm 1$  for the ionization of **1a<sup>+</sup>** were obtained.

The rate of hydrolysis of several other fluoroformamidinium ions with more basic substituents was examined in dilute HCl. The rate of hydrolysis of compounds **1b–d** (Table 1) was found to be pH independent over the range of 0.01–0.1 M HCl, showing that within this concentration range they are fully protonated. Qualitative Brønsted type correlations relating  $k_1$  to the  $\text{p}K_a$  of the free aniline or amine ( $\beta_{\text{dg}}^{\text{ArN}} = -0.31$  and  $\beta_{\text{dg}}^{\text{RN}} = -0.41$ ) indicate that relative to the ground state there is a development of negative charge on both nitrogen atoms at the transition state for spontaneous solvolysis, consistent with an addition–elimination mechanism.

### General acid–base catalysis

Catalysis of the hydrolysis of **1a<sup>+</sup>** by carboxylic acids was investigated. Catalysis by acetate buffer was observed to be linear over the concentration range, 0–0.2 M (Fig. 2). The second-order rate constant for catalysis by acetate ( $k_{\text{Ac}}$ ) was calculated in terms of the fraction of the fluoroformamidinium ion present at the pH concerned. Plots of the rate constants thus obtained against the fraction of the buffer present in the free base form then gave the second-order rate constant for catalysis by the base form of the buffer, as the intercept at 100% free base (Fig. 3). Catalysis by acetate displayed a small solvent isotope effect of  $k_{\text{H}}/k_{\text{D}} = 1.2$ . The uncertainty in this isotope effect is probably close to 20%, reflecting the uncertainty in the equilibrium solvent isotope effect, which was used to calculate it in the manner described above.

The assignment of mechanism based on these observations is ambiguous, thus the possibility of a mechanism of nucleophilic

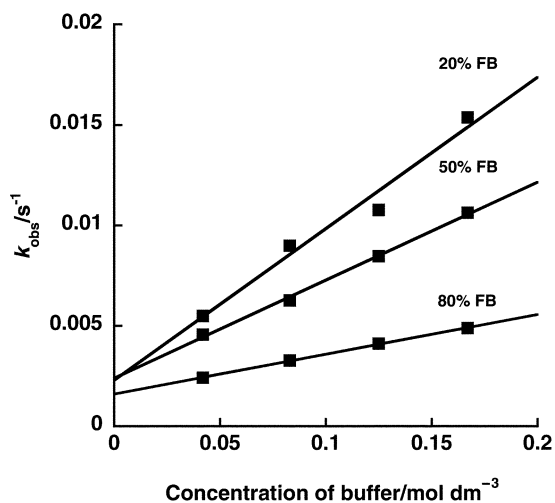


**Fig. 2** Dependence of the first order rate constant  $k_{\text{obs}}$  for the hydrolysis of **1a** on the concentration of acetate buffer at 25 °C and ionic strength 1.0 M (KCl).

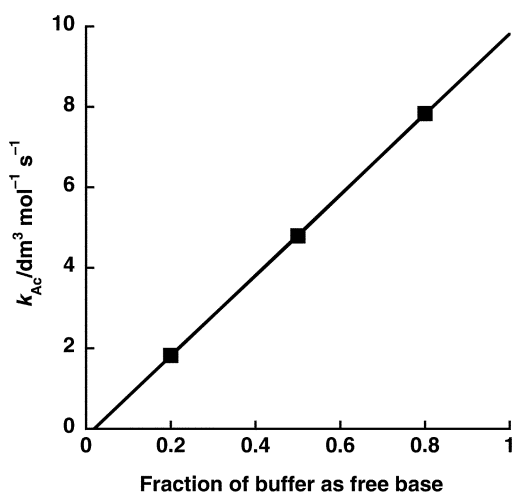
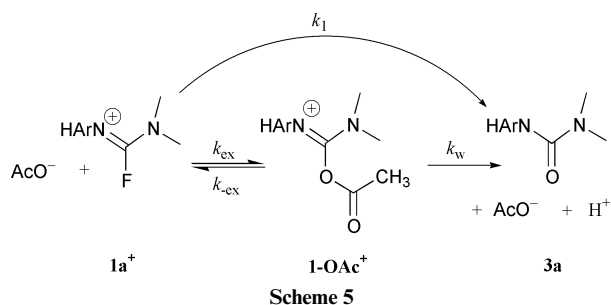


**Fig. 3** Dependence of the second order rate constant  $k_{\text{Ac}}$  for the general base catalysis of the hydrolysis of **1a** against the fraction of the free base component of the acetate buffer (■) at 25 °C and ionic strength 1.0 (KCl). The lines represent the best linear fits through the data.



catalysis by acetate buffer was investigated. The potential intermediate, **1-OAc<sup>+</sup>** (Scheme 5), was synthesized<sup>†</sup> by trapping the iminium ion **2a** with acetate at pH 8,<sup>12</sup> and was tested for kinetic competency. For nucleophilic catalysis to be significant, rapid exchange of fluoride for acetate,  $k_{\text{ex}}$ , must occur followed by rapid hydrolysis of the adduct,  $k_{\text{w}}$ , where  $(k_{\text{ex}}k_{\text{w}}/k_{\text{-ex}} + k_{\text{w}}) > k_1$  (Scheme 5). However, the adduct was found to be kinetically stable for more than 50 half lives under the conditions of the experiment, demonstrating that nucleophilic catalysis is not a viable mechanism of catalysis.

<sup>†</sup>  $\delta_{\text{H}}$  (400 MHz;  $\text{CDCl}_3$ ) 2.12 (3H, s,  $\text{CH}_3$ ), 3.53 (4H, m), 3.62 (4H, m), 7.40 (2H, m), 7.24 (2H, m).

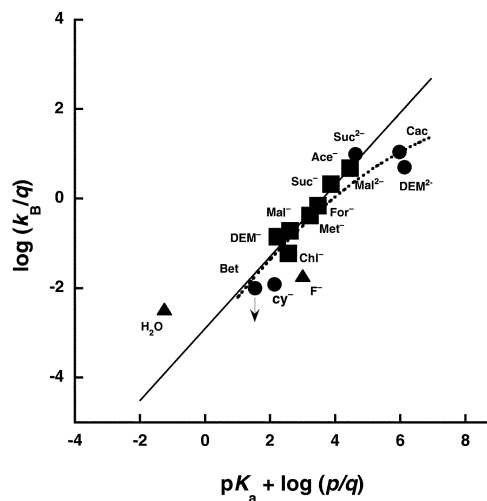


**Fig. 4** Brønsted plot for general base catalyzed hydrolysis of **1a**<sup>+</sup> showing the dependence of  $\log(k_{\text{B}}/q)$  for the general base catalysis of **1a**<sup>+</sup> on the  $\text{p}K_{\text{a}} + \log(p/q)$  of the conjugate acid of the catalyst at 25 °C and ionic strength 1.0 M (KCl). The solid line represents the limiting Brønsted line through the substituted acetate monoanions (■)  $k_{\text{B}}/q = -2.83 + 0.84(\text{p}K_{\text{a}} + \log(p/q))$ . The dashed line corresponds to a plot where,  $p_{\text{x}} = 0.1$  (see reference 26). The data are selected from Table 2.

Catalysis, which was linear with buffer concentration, was demonstrated for a series of oxyacids, which were analyzed in an identical way to acetate. The catalysis was attributed to a mechanism of general acid–base catalysis (Table 1). Cyanoacetate displayed only a moderate rate enhancement over the uncatalyzed reaction, while catalysis by betaine was undetectable at the pH of the experiment. Examination of a statistically corrected Brønsted plot (Fig. 4) reveals that the dependence of  $k_{\text{B}}$  on the experimentally determined  $\text{p}K_{\text{a}}$  of the catalyst is non-linear. This is most apparent if a line with a Brønsted coefficient of  $\beta = 0.80$  is drawn through the carboxylate monoanions ( $\text{p}K_{\text{a}}$  2.22–5.52, filled squares) (excluding betaine and cyanoacetate) as shown in Fig. 4. Several catalysts, most notably betaine, cyanoacetate, fluoride, cacodylate, and dimethylmalonate dianion, fall below the extrapolated plot through the carboxylates. Furthermore, no catalysis was detected for carbonate, hydroxide, 50% free base MES (3-morpholinopropanesulfonic acid) or the monocation of DABCO (1,4-diazabicyclo[2.2.2.]octane) (50% free base). At high pH spontaneous solvolysis of **1a**,  $k_0$ , which is kinetically equivalent to hydroxide ion catalyzed hydrolysis of **1a**<sup>+</sup>, dominates the kinetics. Catalysis by buffers that fall significantly below the limiting line for carboxylates therefore may not be observed due to competition by  $k_0$ . This presumably accounts for the lack of catalysis observed for carbonate, hydroxide, MES and DABCO.

The fact that the point representing water lies some thirty-fold above the Brønsted extrapolation suggests that the uncatalyzed reaction proceeds by an alternative mechanism.

#### Addition of nucleophiles

While a nucleophilic mechanism of catalysis was ruled out for acetates, more polarizable nucleophiles do add directly to **1a**<sup>+</sup>. For example, azide and thiol nucleophiles ( $\text{p}K_{\text{a}}$  3.2 to 10.25) were found to react with **1a**<sup>+</sup> directly, according to the rate law of eqn. (3) (Table 3).

$$k_{\text{nuc}} = k_{\text{n}}[\text{SH}^+] \quad (3)$$

## Discussion

### Fluoroformamidinium ions

Fluoroformamidinium ions **1a–d**, which readily undergo spontaneous hydrolysis (Table 1) are formed at low pH through the

**Table 2** General base catalysis of the hydrolysis of **1a**<sup>+</sup> at 25 °C and ionic strength 1.0 M (KCl)

Catalyst	Conc./M	pL	Base Ⓢ	$k_{\text{cat}}/\text{M}^{-1}\text{s}^{-1}$	$k_{\text{B}}/\text{M}^{-1}\text{s}^{-1}$
Diethylmalonate	0.1–0.6	2.22	0.5	0.1	0.28
Diethylmalonate	0.25–0.75	2.87	0.8	0.08	
Cyanoacetate	0.042–0.17	2.35	0.5	0.0084	0.024
Cyanoacetate	0.042–0.17	2.50	0.5	0.027	0.12
Cyanoacetate	0.042–0.17	3.24	0.8	0.019	
Malonate	0.05–0.2	2.01	0.2	0.057	0.38
Malonate	0.05–0.2	2.61	0.5	0.093	
Malonate	0.05–0.2	3.23	0.8	0.087	
Fluoride	0.08–0.33	3.00	0.5	0.0096	0.019
Methoxyacetate	0.042–0.17	2.63	0.2	0.062	0.84
Methoxyacetate	0.042–0.17	3.27	0.5	0.060	
Methoxyacetate	0.042–0.17	3.95	0.8	0.030	
Formate	0.17–0.83	3.56	0.5	0.081	1.4
Formate	0.17–0.83	4.20	0.8	0.025	
Succinate	0.05–0.25	3.31	0.2	0.17	4.19
Succinate	0.1–0.5	3.87	0.5	0.16	
Succinate	0.1–0.5	4.30	0.8	0.12	
Acetate	0.042–0.17	3.95	0.2	0.076	10.1
Acetate	0.042–0.17	4.54	0.5	0.053	
Acetate	0.042–0.17	5.18	0.8	0.020	
Acetate (D <sub>2</sub> O)	0.042–0.17	4.53	0.2	0.087	6.84
Acetate (D <sub>2</sub> O)	0.042–0.17	5.13	0.5	0.053	
Acetate (D <sub>2</sub> O)	0.042–0.17	5.52	0.7	0.033	
Malonate	0.08–0.3	5.03	0.5	0.035	19.6
Succinate	0.08–0.3	5.22	0.5	0.048	39.5
Cacodylate	0.17–0.67	5.18	0.1	0.0056	22
Diethylmalonate	0.03–0.3	6.11	0.2	0.0018	20.1
Diethylmalonate	0.03–0.3	6.72	0.5	0.0009	
Diethylmalonate	0.03–0.3	7.38	0.8	0.00024	
Carbonate	0.03–0.3	9.65	0.5	—	$<2 \times 10^4$ <sup>a</sup>
Hydroxide	—	—	—	—	$<4.4 \times 10^8$ <sup>b</sup>

<sup>a</sup> Calculated from the  $\text{p}K_{\text{a}}$  of  $\text{HCO}_2^-$  and **1a**<sup>+</sup> and from  $k_0$  for the solvolysis of **1a**. <sup>b</sup> Calculated from the  $\text{p}K_{\text{a}}$  of water and **1a**<sup>+</sup> and from  $k_0$  for the solvolysis of **1a**.

**Table 3** Nucleophilic addition to **1a**<sup>+</sup> at 25 °C and ionic strength 1.0 M (KCl)

Nucleophile	$\text{p}K_{\text{a}}$	Concentration	$k_{\text{nuc}}/\text{M}^{-1}\text{s}^{-1}$ <sup>a</sup>
Water	–1.7	55 000	$4.4 \times 10^{-5}$
Azide <sup>b</sup>	4.72	3.3–16.7	1200
Acetate	4.76	42–170	<1
Thioacetate <sup>b</sup>	3.20	6.7–26.7	770
Methylthioglycolate <sup>c</sup>	9.40	3.3–13.3	180 000
Mercaptoethanol <sup>c</sup>	9.61	50–200	310 000
Thioglycolate <sup>d</sup>	10.25	17–68	660 000

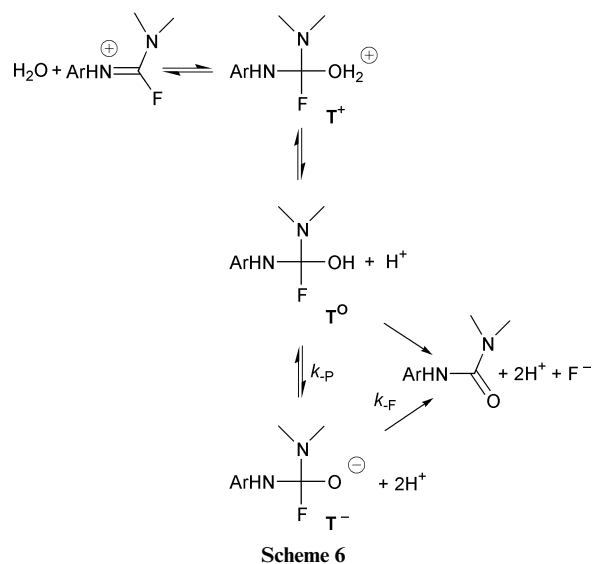
<sup>a</sup> Determined from the observed second-order dependence of product formation and from the concentration of **1a**<sup>+</sup> at each pH. <sup>b</sup> In 0.083 M 50% FB acetate pH 4.58. <sup>c</sup> In 0.05 M 10% FB phosphate, pH 5.44. <sup>d</sup> In 0.083 M 50% FB carbonate pH 9.47. The concentration of thioglycolate dianion was calculated using the  $\text{p}K$  for thioglycolate of 10.25.

protonation of the imidine nitrogen atom of the corresponding fluoroformamidine. The hydrolysis of **1a**<sup>+</sup> to give the corresponding urea was found to be subject to buffer catalysis by carboxylates ( $\text{p}K_{\text{a}}$  2.22–5.52). Catalysis was detected because, unlike more polarizable nucleophiles, such as azide and thiolates, which displace fluorine readily from **1a**<sup>+</sup> (Table 3), the direct addition of carboxylate anions to **1a**<sup>+</sup> does not compete with hydrolysis. A similar selectivity between water and carboxylates was seen for the imidinium cation, **2a**,<sup>12</sup> which reacted with water some 10<sup>6</sup>-fold faster. This reflects the remarkable insensitivity of carbocation selectivity to carbocation stability that has been noted before.<sup>14</sup>

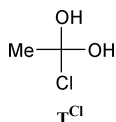
#### Tetrahedral addition intermediates

Several kinetically equivalent mechanisms are consistent with fluoroformamidinium ion hydrolysis. These include fully concerted mechanisms with no intermediate and stepwise

mechanisms that proceed through a tetrahedral addition intermediate. While tetrahedral addition intermediates have been proposed for the hydrolysis of acyl halides<sup>15</sup> and are common at the acyl level of oxidation little information exists on the stability of tetrahedral fluoro-addition intermediates. For the hydrolysis of fluoroformamidinium ions the lifetime of tetrahedral addition intermediate **T**<sup>0</sup>, which lies on the reaction pathway (Scheme 6) must be considered. A comparison with the

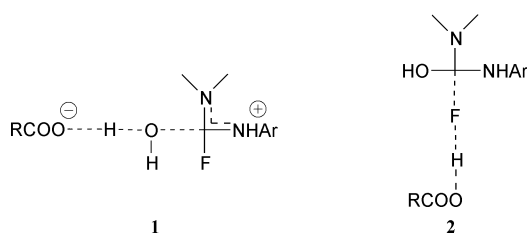


mechanism of solvolysis of acyl chloride, which proceeds through the neutral addition intermediate **T**<sup>Cl</sup>, in aqueous solution is useful.<sup>15</sup> The similarity between **T**<sup>Cl</sup> and **T**<sup>0</sup> suggests that it is reasonable to propose that **T**<sup>0</sup>, which is neutral, has a significant ( $>10^{-13}$  s) lifetime in aqueous solution.

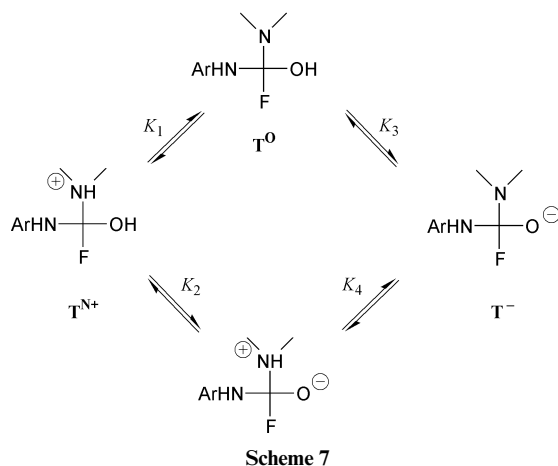


### General acid–base catalysis

Two kinetically equivalent stepwise mechanisms for general base catalysis of the hydrolysis of fluoroformamidinium ions proceed through transition states **1** and **2**. These transition states represent class n mechanisms, in which the catalyst abstracts a proton from the attacking water molecule **1** or donates a proton to the leaving fluoride **2**, which is the nucleophile when the reaction proceeds in the reverse direction. As  $\text{T}^{\ominus}$  is expected to have a significant lifetime a fully concerted mechanism of proton transfer and leaving group expulsion is unlikely for the hydrolysis of fluoroformamidines. A stepwise addition–elimination mechanism is therefore assigned.



While protonation of fluoride by a specific or general acid has been proposed previously,<sup>16</sup> it is predicted that fluoride is a sufficiently good leaving group that for the assigned stepwise addition–elimination through,  $\text{T}^{\ominus}$ , water attack, **1**, is rate limiting. The observation of buffer catalysis over the pH range of pH 2.01–7.38 supports this view, because the  $\text{p}K_{\text{a}}$  of  $\text{T}^{\ominus}$  is estimated to be 6.8 (see Experimental section). Therefore it is anticipated that near pH 7 product formation from  $\text{T}^{\ominus}$  will proceed by rapid deprotonation, to give  $\text{T}^{-}$ , followed by prompt expulsion of fluoride (Scheme 6). This pathway will not be subjected to catalysis through a transition state of the stoichiometry indicated in the rate law and thus fluoride elimination is unlikely to be the rate-limiting step. Expulsion of fluoride from the tautomer  $\text{T}^{\text{N}+}$  (Scheme 7) can also be discounted, because its estimated  $\text{p}K_{\text{a}}$  is 2.38.



Scheme 7

The small solvent isotope effects of  $k_{\text{H}}/k_{\text{D}} = 1.2 \pm 0.2$  for general base catalysis of the addition of water to  $\text{1a}^+$  by several substituted acetates and the Brønsted coefficient of  $\beta = 0.80$  are consistent with slight stretching of an O–H bond in a mechanism in which catalysis occurs through a fully concerted mechanism where the proton is ‘in flight’ in the transition state or hydrogen-bonding of the developing positive charge ‘on’ the attacking water in the transition state.<sup>17</sup> The small isotope effect may result from the asymmetric nature of **1** for proton

transfer<sup>18</sup> which is supported by the Brønsted coefficient, or coupling to C–O bond covalency changes,<sup>19</sup> or because it lies in a potential well.<sup>20</sup> Class n mechanisms in other systems, such as the addition of hydroxy nucleophiles to iminium ions,<sup>21</sup> to phenylethyl carbocations,<sup>22</sup> to orthocarbonates<sup>23</sup> or the hydrolysis of acetals<sup>24</sup> typically exhibit smaller values of  $\beta$  indicating that the proton lies closer to the hydroxylic nucleophile/leaving group in the transition state. In these cases structure–reactivity relationships have provided very good evidence that these reactions are concerted, with movement of both the proton and heavy atoms in the transition state. It is reasoned that in the present case proton transfer within a hydrogen-bonded intermediate species,  $\text{RCOO}^{-} \cdot \text{T}^{\oplus}$ , in which the difference in  $\text{p}K_{\text{a}}$  between the catalyst and the intermediate is *ca.* 16 units, enforces a concerted reaction. The extensive transfer of the proton to the carboxylate catalyst in **1** possibly reflects the resistance of the fluoroformamidinium ions to hydrolysis, compared to other carbocations. The value of  $a = 0.45$  for the expulsion of ROH to give an amidinium ion is consistent with this observation.<sup>25</sup>

Although the Brønsted plot (Fig. 4) through the seven monoanionic carboxylates fits a slope of  $\beta = 0.80$ , several catalysts deviate below this line, suggesting that there may be some downward curvature in the plot. While cyanoacetate displays weak catalysis, which is barely detectable, catalysis by betaine is not detectable at the pH of the experiment and thus only an upper limit is reported. This curvature could be the result of a number of factors which include 1) a change in rate limiting step, 2) a ‘Hammond effect’ on the proton transfer component of the reaction, that results in a change in transition-state structure with increasing  $\text{p}K_{\text{a}}$  of the base catalyst, 3) solvation effects or 4) differences in catalyst structures.

A change in rate limiting step from water attack to fluoride expulsion with increasing basicity of the catalyst could result in non-linearity of a Brønsted plot. Plots of  $k_{\text{B}}$  against buffer concentration were linear for all the buffers examined, suggesting that a change in the rate limiting step is not the source of the non-linearity for cacodylate or DEM dianion. However, a change in rate-limiting step cannot be excluded for carbonate or hydroxide for which no catalysis was detected due to competition from the unimolecular solvolysis of **1a**,  $k_0$ .

A Hammond effect for a class n mechanism can be described by the coefficient,  $p_x = d\beta/d\text{p}K_{\text{BH}^+}$ , where a positive value of  $p_x$  corresponds to a decrease in  $\beta$  with increasing basicity of the catalyst.<sup>26</sup> While the structure of the transition state for general base catalyzed addition of water or alcohols to electron deficient centers is sensitive to changes in structure there is often no significant curvature of the Brønsted plot.<sup>27</sup> In other words the  $p_x$  coefficient is typically close to zero. However, this may not always be the case. If, for example, the proton is included in Brønsted plots for general acid catalysis of orthocarbonate hydrolysis,<sup>23</sup> significant downward curvature is inferred and in this case,  $p_x > 0$ . The dashed line in Fig. 4 is presented merely as a guide as to how much curvature may be expected in a Brønsted plot when the interaction coefficient has the value of  $p_x = 0.1$ . While such a Hammond effect would satisfactorily account for the negative deviations of cacodylate, hydroxide and carbonate from the statistically corrected plot through the carboxylates, other factors must be considered.

It is well known that non-linear Brønsted plots can also result from solvation effects, which have been noted for a number of processes that include proton transfer at carbon<sup>28</sup> and the addition of oxyanion<sup>29</sup> nucleophiles to esters. However, Brønsted correlations for proton transfer reactions between electronegative atoms are generally linear, possibly because unlike transfer at carbon they often proceed through solvent molecules.<sup>30</sup> While it is fairly safe to assume that desolvation effects of weakly basic carboxylates ( $\text{p}K_{\text{a}} < 8$ ) are not likely to be kinetically significant, it cannot be ruled out for hydroxide, carbonate and the highly solvated fluoride anion.

In summary, differences in the structure between catalysts can lead to significant scatter of Brønsted plots and could account for the deviations of such ions as fluoride, betaine and DABCO from the line through the carboxylates. While hydroxide is rarely found to negatively deviate from Brønsted correlations for general base catalysis involving electronegative atoms it is possible that both a structural and Hammond effect could contribute to such a deviation from the line through the carboxylates. ‡

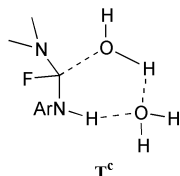
### Spontaneous hydrolysis

The rate constant for water deviates positively from the Brønsted plot ( $\delta = 0.80$ ) for general base catalysis of the addition of water by a factor of ~30 fold, which suggests that an alternative mechanism or transition state structure may exist for the uncatalyzed hydrolysis reaction.

If the Brønsted parameter of  $\beta = 0.80$  is a measure of the extent of proton transfer to a water molecule at the transition state a solvent isotope effect that approaches the maximum expected value of 3.05 for the formation of a solvated proton should be observed for a class n mechanism **1**.<sup>31</sup> In fact a secondary solvent isotope effect of 2.5 is predicted using the Brønsted coefficient as a measure of the degree of proton transfer at the transition state.<sup>32</sup> This is greater than the observed isotope effect, which presumably also includes a contribution from a primary isotope effect. Thus, the observed isotope effect of  $k_H/k_D = 1.7$  also supports the assignment of a transition state structure for the uncatalyzed reaction that differs from **1**.

The Brønsted type coefficient of  $\beta_{\text{ag}}^{\text{ArN}} = -0.3\delta$  indicates that C–O bond formation is early, *ca.* 30%, at the transition state. A reasonable assignment consistent with this and the observed isotope effect of  $k_H/k_D = 1.7$  is a cyclic transition state (**T<sup>c</sup>**) where several O–H bonds have undergone a small degree of stretching.

Another possibility is that the stepwise addition of water to give **T<sup>+</sup>** is concurrent with the class n mechanism. While rare, concurrent stepwise and concerted mechanisms have been observed for some class n mechanisms.<sup>33</sup> Such a mechanism requires that the intermediate **T<sup>+</sup>** has a sufficiently long lifetime in aqueous solution that it can be said to exist.<sup>33</sup>



### Enzyme reaction

While studying the mechanism of hydrolysis of 1,3-diphenylimidazolium ion in the late 1960's Robinson provided direct evidence for the existence of a tetrahedral intermediate.<sup>4</sup> This and other studies<sup>5–10</sup> supported the notion that the rate-limiting step for formamidine hydrolysis is the breakdown of a tetrahedral intermediate. Interestingly, however, the kinetics of the hydrolysis of methenyltetrahydrofolic acid itself appear to be more complex than the model studies, because an apparent change in rate-limiting step is seen as buffer concentration is varied.<sup>5</sup> The available data support the notion that for the cyclohydrolase catalyzed hydrolysis of methenyltetrahydrofolic acid both formation and breakdown of a tetrahedral intermediate require the participation of a catalytic residue.

‡ The deviation from the limiting line through the monoanionic carboxylates is more than ten-fold and therefore is not due to the approach of the hydroxide reaction to the diffusion controlled limit (See Table 1).

§ The reference reaction for  $\beta_{\text{ag}}^{\text{ArN}}$  is the experimentally measured dependence of  $K_a$  for the ionization of the fluoroformamidinium ions on the  $pK_a$  of the aniline,  $\beta_{\text{eq}} = 0.91$  (see Table 1).

Interestingly, cyclohydrolase appears to possess only one active site residue, Lys-56, which could function as a general acid or base.<sup>34</sup> Accordingly, it is proposed that Lys-56 facilitates general base catalyzed addition of water to methenyltetrahydrofolic acid through a class n mechanism. The mechanism by which the intermediate breaks down is currently unknown and could proceed by at least one of two different kinetically equivalent mechanisms that have been proposed in model studies.<sup>5–10</sup>

### Conclusions

The solvent isotope effects and the Brønsted correlation are consistent with a concerted class n mechanism of catalysis in which concerted proton transfer in the transition state provides catalysis of the addition of water to the formamidinium ion. It is predicted that proton transfer within a hydrogen-bonded intermediate species,  $\text{RCOO}^- \cdot \text{T}^+$  in which the difference in  $pK_a$  between the catalyst and the intermediate is *ca.* 16 units, enforces a concerted reaction. The uncatalyzed mechanism appears to proceed through a different mechanism, possibly through a concerted cyclic transition state or a stepwise mechanism of addition and proton transfer.

### Experimental

#### Synthetic methods

The substrates used throughout this study were prepared essentially as previously described.<sup>12</sup>

#### Materials

Cacodylic acid, sodium azide, potassium fluoride, potassium carbonate and thioacetate were the best commercially available grades and were used without further purification. Betaine, cyanoacetate, chloroacetate, methoxyacetate, acetate and formate were recrystallized as their potassium salts from aqueous ethanol. Methyl thioglycolate, mercaptoethanol and thioglycolate were distilled prior to use and stored at 4 °C under nitrogen for up to two weeks. Millipore water was used throughout. The  $\text{D}_2\text{O}$  used throughout this study was obtained as 99.99% isotopically pure from Cambridge Isotopes. DCl (99.99% isotopically pure) and KOD (98+% isotopically pure) were obtained from Aldrich and were titrated against a standard before use.

#### Kinetic methods

The reaction solutions at ionic strength of  $1.0 \text{ mol dm}^{-3}$  (KCl) were prepared in  $3000 \text{ mm}^3$  quartz cells from stock solutions. They were equilibrated to 25 °C, before the addition of *ca.*  $5 \text{ mm}^3$  of a stock solution of substrate, and the recording commenced. For reactions with half-lives less than 30 s the substrate was dissolved in  $\text{H}_2\text{O}$  before the buffer or a solution of HCl was added and the recording commenced. The concentration of buffer was >100 times that of the substrate (0.05–0.1 mM), so that pseudo first order conditions were maintained. Standard conditions were 25 °C at ionic strength  $1.0 \text{ mol dm}^{-3}$ , maintained with potassium chloride. All pH measurements were made under the conditions of the kinetic experiment using an Orion Research Digital pH meter with a 611 Corning semi micro combination electrode. The pD of solutions in  $\text{D}_2\text{O}$  was measured using the same electrode, which had been standardized against (protium) standard buffers and was taken to be 0.4 units above the reading of the pH meter.<sup>35</sup> The reactions were studied by monitoring at the wavelength that gave the largest change in absorbance and the data were recorded on a computer attached directly to the spectrophotometer. Data were analyzed on a Macintosh Powerbook computer using Kaleidagraph. Semilogarithmic plots of  $A_t - A_{\text{inf}}$  against time were

linear for more than three half lives in all cases. Rate constants for catalysis by buffer and for reaction with water were determined from the slopes and intercepts of plots of  $k_{\text{obs}}$  against concentration of buffer respectively. The solvent isotope effects  $k_{\text{H}}/k_{\text{D}}$  for catalysis by several substituted acetates were obtained using the slopes of plots of  $k_{\text{obs}}$  against buffer concentration. A correction was made for the different fractions of  $\mathbf{1a}^+$  in  $\text{H}_2\text{O}$  and  $\text{D}_2\text{O}$  using the measured equilibrium isotope effect. The error in this value is estimated to be 20%.

### Product analysis

**Hydrolysis.** The products of the reactions were analyzed by examining the changes in the ultraviolet spectra under the standard kinetic conditions and by examining the  $^1\text{H}$  NMR spectra of isolated products as described previously.<sup>12</sup> Hydrolysis of  $\mathbf{1a}$  in aqueous solution gave the urea in the pH 0–14 range. All derivatives  $\mathbf{1b-d}$  display similar changes in their ultraviolet spectra upon hydrolysis, which are characterized by two isosbestic points. The hydrolysis of the corresponding chloro compounds gives the same urea products upon rapid hydrolysis. The product of carboxylate, cacodylate and phosphate catalyzed reactions is the urea which is identified by the identical change in the ultraviolet spectrum.

**With nucleophiles.** Analysis of the ultraviolet spectral changes on the addition of azide, thioacetate, methyl thioglycolate, mercaptoethanol and thioglycolate indicate that these anions form stable adducts with  $\mathbf{1a}$  under the standard kinetic conditions. The ultraviolet spectra of adducts are identical to the products of the reactions between  $\mathbf{1a}$  and the anions under conditions which favor trapping of the imidinium cation,  $\mathbf{2a}$ .

### Estimating acid dissociation constants

The  $\text{p}K_{\text{a}}$  values of the intermediates in Scheme 7 were estimated following a similar procedure to Fox and Jencks<sup>36</sup> which is explained in the appendix of the book by Page and Williams.<sup>37</sup> Initial  $\text{p}K_{\text{a}}$  values for model compounds were taken from ref. 38. Inductive effects were estimated using  $\sigma_{\text{I}}$  values and  $\rho = -9.1$  which is appropriate for a X–C–Y system.<sup>37</sup>

**Estimation of  $\text{p}K_1$ .**  $\text{p}K_1$  was estimated starting from the  $\text{p}K_{\text{a}}$  for *N*-methylmorpholine of 7.41. The calculation gives  $\text{p}K_1 = 7.41 - [9.1 \times (0.54 + 0.30 + 0.24)] = -2.42$ .

**Estimation of  $\text{p}K_2$ .**  $\text{p}K_2$  was estimated starting from the  $\text{p}K_{\text{a}}$  for  $\text{CH}_3\text{CH}_2\text{OH}$  of 16. The calculation gives  $\text{p}K_2 = 16 - [9.1 \times (0.54 + 0.30 + 0.7)] = 2.0$ .

**Estimation of  $\text{p}K_3$ .**  $\text{p}K_3$  was estimated starting from the  $\text{p}K_{\text{a}}$  for  $\text{CH}_3\text{CH}_2\text{OH}$  of 16. The calculation gives  $\text{p}K_3 = 16 - [9.1 \times (0.54 + 0.30 + 0.17)] = 6.8$ .

**Estimation of  $\text{p}K_4$ .** The value of  $\text{p}K_4$  is given by  $\text{p}K_1 + \text{p}K_3 - \text{p}K_2 = 2.38$ . Ionization of the hydroxy group stabilizes the development of a positive charge on nitrogen by 4.8 units (compare  $\text{p}K_4$  and  $\text{p}K_1$ ) as previously noted.<sup>36</sup>

The  $\text{p}K_{\text{a}}$  of  $\mathbf{T}^+$  in Scheme 6 was estimated starting from the  $\text{p}K_{\text{a}}$  for  $\text{HOH}_2^+$  of  $-2$ . The calculation gives  $\text{p}K_{\text{a}} = -2 - [9.1 \times (0.54 + 0.30 + 0.17)] = -11.2$ .

### Acknowledgements

Initial experiments were performed while K. N. D. was a post-doctoral fellow in the laboratory of W. P. Jencks. This research

was supported by a grant from the Welch Foundation (F-1390) and from the National Institutes of Health (GM-59802) to K. N. D.

### References

- 1 D. Voet and J. G. Voet, *Biochemistry*, John Wiley, New York, 1995.
- 2 R. H. DeWolfe, *J. Am. Chem. Soc.*, 1960, **82**, 1585; R. H. DeWolfe, *J. Am. Chem. Soc.*, 1964, **86**, 864.
- 3 R. H. DeWolfe, in *Chemistry of Amidines*, ed. S. Patai, Wiley-Interscience, New York, p. 349.
- 4 D. R. Robinson, *Tetrahedron Lett.*, 1968, 5007; D. R. Robinson, *J. Am. Chem. Soc.*, 1970, **92**, 3138.
- 5 D. R. Robinson and W. P. Jencks, *J. Am. Chem. Soc.*, 1967, **89**, 7088; D. R. Robinson and W. P. Jencks, *J. Am. Chem. Soc.*, 1967, **89**, 7098.
- 6 S. J. Benkovic, *Acc. Chem. Res.*, 1978, **11**, 314.
- 7 M. I. Page, P. Webster and L. Ghosez, *J. Chem. Soc., Perkin Trans. 2*, 1990, 813.
- 8 A. Chandler, A. F. Hegarty and M. T. McCormack, *J. Chem. Soc., Perkin Trans. 2*, 1980, 1318.
- 9 M. I. Page, P. Webster and L. Ghosez, *J. Chem. Soc., Perkin Trans. 2*, 1990, 805.
- 10 B. A. Burdick, P. A. Benkovic and S. J. Benkovic, *J. Am. Chem. Soc.*, 1977, **99**, 5716.
- 11 W. P. Jencks, *Acc. Chem. Res.*, 1976, **72**, 705.
- 12 K. N. Dalby and W. P. Jencks, *J. Am. Chem. Soc.*, 1997, **119**, 7271.
- 13 J. Oszczapowicz and J. Jaroszevska-Manaj, *J. Chem. Soc., Perkin Trans. 2*, 1991, 1318; J. Oszczapowicz and E. Raczniska, *J. Chem. Soc., Perkin Trans. 2*, 1984, 1643.
- 14 C. D. Ritchie, *Acc. Chem. Res.*, 1972, 348.
- 15 R. J. E. Talbot, in *Comprehensive Chemical Kinetics, X, The Hydrolysis of Carboxylic Acid Derivatives*, 1972, p. 287.
- 16 N. S. Banait and W. P. Jencks, *J. Am. Chem. Soc.*, 1991, **113**, 7958.
- 17 P. E. Dietze and W. P. Jencks, *J. Am. Chem. Soc.*, 1989, **111**, 340.
- 18 F. Westheimer, *Chem. Rev.*, 1961, **61**, 265.
- 19 K. A. Engdahl, H. Bivehed, P. Ahlberg and W. H. Saunders, Jr., *J. Am. Chem. Soc.*, 1983, **105**, 4767.
- 20 C. G. Swain, D. A. Kuhn and R. L. Schowen, *J. Am. Chem. Soc.*, 1965, **87**, 1553.
- 21 N. Gravitz and W. P. Jencks, *J. Am. Chem. Soc.*, 1973, **96**, 507.
- 22 J. P. Richard and W. P. Jencks, *J. Am. Chem. Soc.*, 1984, **106**, 1396.
- 23 P. Kandanarachchi and M. Sinnott, *J. Am. Chem. Soc.*, 1994, **116**, 5601.
- 24 B. Capon and K. Nimmo, *J. Chem. Soc., Perkin Trans. 2*, 1975, 1113.
- 25 H. F. Gilbert and W. P. Jencks, *J. Am. Chem. Soc.*, 1982, **104**, 6769.
- 26 D. A. Jencks and W. P. Jencks, *J. Am. Chem. Soc.*, 1977, **99**, 7948.
- 27 W. P. Jencks, *Chem. Rev.*, 1985, **85**, 511.
- 28 D. Hupe and D. Wu, *J. Am. Chem. Soc.*, 1977, **99**, 7653.
- 29 D. J. Hupe, D. Wu and P. Shepperd, *J. Am. Chem. Soc.*, 1977, **99**, 7659.
- 30 E. Grunwald and D. Eustace, in *Proton Transfer Reactions*, eds. E. F. Caldin and V. Gold, Chapman and Hall, London, UK, 1975, p. 103.
- 31 J. Albery in *Proton Transfer Reactions*, eds. E. F. Caldin and V. Gold, Chapman and Hall, London, UK, 1975, p. 263.
- 32 D. A. Winey and E. R. Thornton, *J. Am. Chem. Soc.*, 1975, **97**, 3102.
- 33 J. L. Palmer and W. P. Jencks, *J. Am. Chem. Soc.*, 1980, **102**, 6466; S. Rosenberg, S. M. Silver, J. M. Sayer and W. P. Jencks, *J. Am. Chem. Soc.*, 1974, **96**, 7986.
- 34 A. Schmidt, H. Wu, R. E. MacKenzie, V. J. Chen, J. R. Bewly, J. E. Ray, J. E. Toth and M. Cygler, *Biochemistry*, 2000, **39**, 6325.
- 35 P. K. Glasoe and F. A. Long, *J. Phys. Chem.*, 1960, **64**, 188.
- 36 J. P. Fox and W. P. Jencks, *J. Am. Chem. Soc.*, 1974, **96**, 1436.
- 37 M. Page and A. Williams, *Organic and Bioorganic Mechanisms*, Addison Wesley Longman, Harlow, England, 1997.
- 38 W. P. Jencks and J. Regenstein, *Handbook of Biochemistry and Molecular Biology*, ed. H. A. Sober, CRC Press, Cleveland, 2nd edn., 1970.